Effect of viscosity and density ratios on two drops rising side-by-side

Mounika Balla, Sivanandan Kavuri, Manoj Kumar Tripathi[†], Kirti Chandra Sahu,[*] and Rama Govindarajan[††]
Department of Chemical Engineering, Indian Institute of Technology Hyderabad, Sangareddy 502 285, Telangana, India
[†]*Indian Institute of Science Education and Research Bhopal 462 066, Madhya Pradesh, India*
[††]*International Centre for Theoretical Sciences, Shivakote, Bengaluru 560089, India.*

We study the dynamics of a pair of initially spherical drops rising side-by-side in a surrounding, denser, fluid. Our primary focus is on liquid-liquid systems, and a range of viscosity and density ratios are explored by three-dimensional numerical simulations. Interesting dynamics are reported, which cannot be extrapolated from previously known dynamics of gas-liquid systems. Similar to two air bubbles though, we find that two liquid drops move away from each other as they rise, in cases where a single drop would rise vertically. A pair of light drops always remains in two-dimensional motion, and higher drop viscosity increases the tendency of wobbling. This is in contrast with the dynamics of a single drop that follows a highly three-dimensional trajectory at very low drop viscosity, but is restricted to two-dimensional motion at higher drop viscosity. On the other hand, a pair of heavier drops displays three-dimensional behaviour at low drop viscosity and two-dimensional behaviour at high viscosity. We find that a pair of drops is far less sensitive to viscosity contrast than a single drop is, in our parameter range. In contrast to gas-liquid systems, where shape change of the bubble was tied to nonlinear dynamics of the trajectory, we find in liquid-liquid systems that interesting drop trajectories can occur without corresponding large shape changes. It is found that the separation distance between the drops exhibits a non-monotonic trend with an increase in the density ratio. The physical reason for this non-monotonic trend is simple and explained by inspecting the velocity components.

[*] ksahu@iith.ac.in

I. INTRODUCTION

The complex interaction of air bubbles in a liquid has been extensively studied in the past due to its relevance in many industrial applications (see for instance Refs. [1–3]). The size distribution of bubbles and the associated hydrodynamic behaviour greatly influence the heat and mass transfer, and rate of chemical reaction in bubble column reactors, bio-reactors, microfluidics, etc. [4, 5]. The dynamics observed in such applications is very complex and computationally difficult to handle. Experiments also provide useful but only average flow features. Thus, in order to improve the fundamental understanding of these complex flows, model problems, e.g., the rising dynamics of a single bubble [6] and that of two initially spherical bubbles rising side-by-side [7–11] or in a line along the vertical axis [12–17], have been considered by several researchers previously. However, the former configuration (dynamics of a single bubble) has been studied in greater detail than the latter one (two bubbles rising side-by-side or in a line along the vertical axis). Moreover, the effect of viscosity and density contrasts on the rise dynamics of two initially spherical bubbles has not been investigated yet. A brief review of the literature on the fluid dynamics of a single bubble and two bubbles rising side-by-side is provided below.

Three dimensionless numbers are generally used to describe the rise dynamics of bubbles and drops, namely, the Galilei number $\left(Ga(\equiv \rho_A g^{1/2} R^{3/2}/\mu_A)\right)$, the Eötvös number, $\left(Eo(\equiv (\rho_A - \rho_B) g R^2/\sigma)\right)$, and the Morton number (Mo) that can also be defined as Eo^3/Ga^4, in addition to the viscosity ratio $(\mu_r(\equiv \mu_B/\mu_A))$ and the density ratio $(\rho_r(\equiv \rho_B/\rho_A))$. Here, R is the initial radius of the bubble/drop, σ is the interfacial tension, and ρ_A, μ_A and ρ_B, μ_B are densities and viscosities of the continuous and dispersed phases, respectively. Some researchers also used Reynolds number, Re (defined using the terminal velocity as the velocity scale, V_s; $Re = V_s \rho_A R/\mu_A$) instead of Ga (defined using a velocity scale equals to $\sqrt{gR}$). For an air bubble rising in water, $\mu_r = 0.017$ and $\rho_r = 10^{-3}$.

Bhaga & Weber [18] conducted systematic experiments on an air bubble rising in aqueous sugar solutions of different concentrations and obtained a region map in Re-Eo_p space that classifies the bubble behaviours in terms of bubble shape and its path. Here, their Eötvös number, Eo_p was defined based on the density of the continuous phase, as $Eo_p = \rho_A g R^2/\sigma = Eo/(1-\rho_r)$. Note that for air-liquid system, as ρ_r is small (10^{-3}), $Eo \approx Eo_p$. However, Haberman & Morton [19] were probably the first to conduct experiments on rising bubbles in viscous liquids. Recently, by conducting three-dimensional numerical simulations, Tripathi *et al.* [20] presented a phase diagram in Ga-Eo_p space for bubble shapes and its trajectories. They [20, 21] identified five different regimes, namely, axisymmetric, skirted, zigzagging/spiralling, peripheral break-up and central breakup. Their phase plot can also include unsteady bubbles, for which there is no terminal velocity. This phase diagram was validated by Sharaf *et al.* [21] experimentally for an air-liquid system. The hydrodynamics of a single bubble in quiescent liquid has also been studied in Refs. [22–24] computationally. The bubble dynamics of interest to the present study lie in (i) the axisymmetric regime at low Eo_p and low Ga, where a bubble maintains its azimuthal symmetry and (ii) the zigzagging/spiralling regime observed at low Eo_p and high Ga, where a bubble rises in a zigzag or a spiral path; commonly known as path instability [25–27]. Here we remark that the above review of the studies on a single bubble/drop rising in a viscous liquid is rather a small subset of a large volume of work conducted on this subject.

We next present the literature associated with pair of bubbles/drops rising side-by-side. The interactions and trajectories of a pair of spherical air bubbles rising side-by-side in liquid have been investigated by several researchers analytically in the Stokes [28] and the potential flow [7, 29] limits. A summary of some previous studies on two bubbles rising side-by-side is provided in Table I, roughly in increasing order of Reynolds number. Broadly, spherical bubbles, which in Stokes flow would rise with constant separation, repel each other at low Reynolds numbers and attract each other at high Reynolds numbers. Legendre *et al.* [7] investigated flow past two spherical bubbles by conducting three-dimensional simulations for a wide range of Reynolds number. They found that when the boundary layer thickness is small as compared to the separation distance between the bubbles, an irrotational mechanism is in operation, and the bubbles are attracted to each other. On the other hand, in the viscous regime (for low Ga), the boundary layers around the bubbles interact with each other resulting in a repulsive force that separates the bubbles. Here, due to the interface boundary condition, downward flow (with respect to the bubble reference frame) past a bubble creates vorticity close to bubble, whose sense is such that upward velocity is induced. When there are two bubbles, at low to moderate Reynolds number, there is a significant asymmetry in the vorticity isocontours, on the two sides of a given bubble. The isocontours of vorticity come closer together within the gap, which locally increases the upward induced velocity, i.e., decreases the net downward velocity. The difference in velocity on the two sides of the bubble is such that a net lift in the direction away from the other bubble, namely a repulsive force, is generated.

Recently, Zhang *et al.* [30] numerically studied two bubbles rising side-by-side for Reynolds numbers ranging from 10 to 700 and demonstrated the influence of vortex interaction on the repelling and attractive motions of the bubbles. Their results are in agreement with Legendre *et al.* [7]. Sanada *et al.* [8] experimentally investigated the dynamics of a pair of bubbles rising side-by-side for moderate and large values of Re. Again they found repulsion at small Reynolds number and attraction at higher Reynolds numbers. In the attracting case, they also identified coalescence and bouncing behaviours for different values of the Weber number $(We \equiv \rho_A V_s^2 R/\sigma)$. Tripathi *et al.* [11] also

References	Flow regime	Initial separation distance (q_0)	Nature of interaction
Legendre *et al.* [7]	$Re = 0.01$-250	2.25-20	Viscous regime (low Re): Repulsion Potential flow regime (high Re): Attraction The transitional Re depends on the value of q_0
Zhang *et al.* [30]	10-700	2.6-8	$Re \lessapprox 50$: Repulsion Higher Re: Attraction
Sanada *et al.* [8]	$Re = 16$ $Re = 163 - 291$	2-5	Repulsion Attraction
Tripathi *et al.* [11]	$Ga = 20$ & 40	3	Repulsion
Duineveld [31]	$Re > 100$	4-10.6	Coalesce ($We < 0.18$) Bounce ($We > 0.18$)
Kok [29, 35]	Potential flow	4-6	Attraction for bubbles rising side by side ($\theta = 90^\circ$)

TABLE I. The behaviour of two air bubbles rising side-by-side in liquids as reported in the literature. Note that in Tripathi *et al.* [11] the corresponding Re values are about the same as those of Ga.

investigated the dynamics of a pair of air bubbles rising in water via three-dimensional numerical simulations in the inertia-dominated regime. Their work was restricted to the repulsive range of Reynolds numbers.They found that interaction between the wakes of the bubbles can cause oscillatory motion/path instability.

Duineveld [31] conducted experiments on a single bubble and a pair of bubbles rising in the same liquid at high Reynolds numbers. Most of these experiments were in the attracting range of Reynolds numbers, and whether the bubbles coalesced or bounced away depended on the Weber number. We note that our study is focussed on moderate values of the Weber number. Kok [29] investigated the trajectories of bubbles theoretically in the potential flow limit and found that bubbles initially placed side-by-side experience an attraction to each other. This early theoretical finding provides the mechanism for the attraction seen at high Reynolds numbers, where the viscous boundary layers around each bubble are thin. We mention in passing that Kok [29] also showed that the sign of the force between the bubbles in potential flow depends on the initial orientation of their line of separation to the vertical.

The literature on bubbles rising in non-Newtonian fluids is vast. While the physics there could be different, we briefly mention a few findings in bubbles rising side by side. Velez-Cordero *et al.* [32] and Islam *et al.* [33] studied the motion of bubbles in shear-thinning fluids for $Re < 10$ and approximately $20 - 100$, respectively. They found repulsive interaction, except when the initial separation and the Reynolds number were large. Thus, the behaviour is qualitatively the same as that in Newtonian fluids [7]. Zenit and Feng [34] in their review noted that bubbles rising side-by-side in a shear-thinning fluid exhibit drafting-kissing-tumbling behaviour, as observed earlier by Velez-Cordero *et al.* [32].

All these studies on single bubble and pairs of bubbles are associated with gas-liquid systems. Although there exist a few studies on a single drop of liquid rising in another liquid (which are reviewed below), to the best of our knowledge, no one has investigated dynamics of a pair of liquid drops rising side-by-side in another immiscible liquid for finite inertia, in spite of the fact the one encounters such liquid-liquid systems in many industrial applications. Many researchers have however investigated solid spheres falling in liquids. For example, allowing two solid spheres to fall side-by-side with a small initial gap in a sedimentation channel, Joseph *et al.* [36] showed that the spheres separated away in a Newtonian surrounding liquid, but attracted each other in a viscoelastic fluid. They remarked that the shear-thinning nature and memory may be responsible for the aggregation of the spheres. We shall see below that the behaviour of liquids rising in other liquids departs both from that of bubbles and also that of solid spheres, since viscosity and density ratios, and well as shape change affect the dynamics.

The viscosity and density ratios of nearly 1650 pairs of fluids used in industries and households are presented in Fig. 1. In the present study, we only consider situations with $\rho_r < 1$, i.e., rising drops. It should be noted that the inclusion of temperature or concentration of some species often changes the viscosity drastically. Such effects along with the consideration of non-Newtonian behaviour of other fluids will give new dimensions to Fig. 1.

Ohta *et al.* [37] investigated rise dynamics of a single drop in a liquid-liquid system. They studied the effect of viscosity and density ratios on drop shape by performing axisymmetric numerical simulations. They found that the viscosity ratio has a significant effect on the rise dynamics for low values of Mo. In another study, Ohta *et al.* [38] investigated a single liquid drop in an immiscible viscous liquid by conducting experiments and three-dimensional numerical simulations using a coupled level-set and volume-of-fluid approach. They found that increasing the viscosity ratio leads to wobbling motion in case of low Mo and low Eo_p. For high values of Eo_p the drop undergoes breakup. Liu *et al.* [39] studied a single liquid drop rising in another liquid by conducting axisymmetric numerical simulation based on a front-tracking approach. They also found that for low Mo, the drop undergoes a sudden change in its topology leading to breakup. Premlata *et al.* [40] numerically investigated the dynamics of an air bubble rising in an

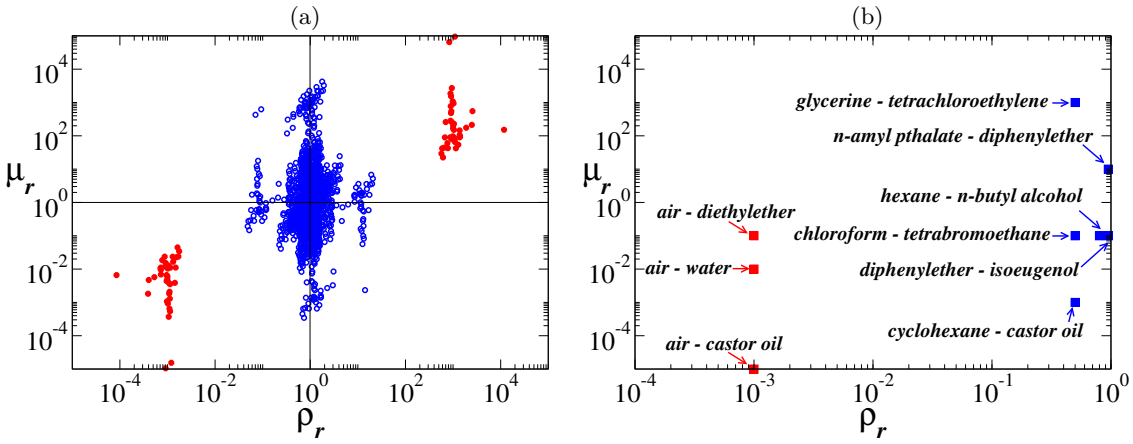

FIG. 1. (a) The density (ρ_r) and viscosity (μ_r) ratios of about 1650 pairs of fluids. Blue (open) and red (filled) symbols represent liquid-liquid and liquid-gas systems, respectively. (b) Some of the fluid pairs considered in the present study.

unconfined quiescent viscosity-stratified medium and found that in contrast to the constant viscosity system, in this case, the bubble undergoes large deformation by forming an elongated skirt that physically separates the wake region from the rest of the surrounding fluid.

As the above literature review shows, the dynamics of a single bubble/drop has been investigated for air-liquid and liquid-liquid systems; however, the dynamics of pair of bubbles rising side-by-side has been investigated for only air-liquid systems. In the present work, we investigate the effect of viscosity and density ratios on the rise dynamics of a pair of drops inside quiescent liquid by conducting three-dimensional numerical simulations. From our previous study [11], we learned about the behaviour of a light and low viscosity pair of drops, but when we increase the density of the drop interesting things start happening. The behaviour becomes more three-dimensional, and better still, this is opposite to what a single drop does. Increasing viscosity makes the drop more spherical but the horizontal separation between the drops still increases. This behaviour is similar to that one observes in case of a pair of solids [41, 42]. Therefore, it is necessary to study the whole parameter space, and a lot needs to be understood in case of a pair of liquid drops rising in other liquids. The present work in an attempt in this direction. The effect of the initial separation distance between the drops has also been studied by Tripathi *et al.* [11]. They found that when the initial separation distance between the drops is small, their trajectories are mere the mirror images of each other. The symmetry in the trajectories of the drops is broken with the increase in their initial separation distance; in this case, one of the drops oscillates gently into the third dimension, whereas the other displays large forays in the spanwise direction. Of course, for very large initial separation distance, the drops can be expected to behave like two independent single drops. In the present study too we observed similar behaviour for different viscosity and density ratios. Thus we only present the results for a fixed value of the initial separation distance between the drops.

The rest of the paper is organized as follows. The details of the problem formulation is provided in Section II. The results are discussed in Section III, and concluding remarks are given in Section IV.

II. FORMULATION

The dynamics of two initially spherical drops (dispersed phase; designated by fluid 'B') of radii R rising side-by-side in a quiescent surrounding medium (continuous phase; designated by fluid 'A') under the action of gravity (g) is investigated via direct numerical simulations of three-dimensional incompressible Navier-Stokes and continuity equations. A schematic diagram of the initial flow configuration is shown in Fig. 2. The fluids are assumed to be Newtonian and incompressible. The viscosity and density of fluid 'A' and fluid 'B' are (μ_A, ρ_A) and (μ_B, ρ_B), respectively, such that $\rho_B < \rho_A$ (drops). A Cartesian coordinate system (x, y, z) is used with the gravity (g) acting in the negative z direction. The initial coordinates of drop '1' and drop '2', as designated in Fig. 2, are $(-q_0/2, 0, z_0)$ and $(q_0/2, 0, z_0)$, respective, wherein $q_0 = 3R_0$ and $z_0 = 7R_0$ are the initial separation distance between the drops and initial height from the bottom of the computational domain. A big computational domain of size $120R \times 120R \times 120R$ is considered so that the boundary effects on the dynamics can be neglected.

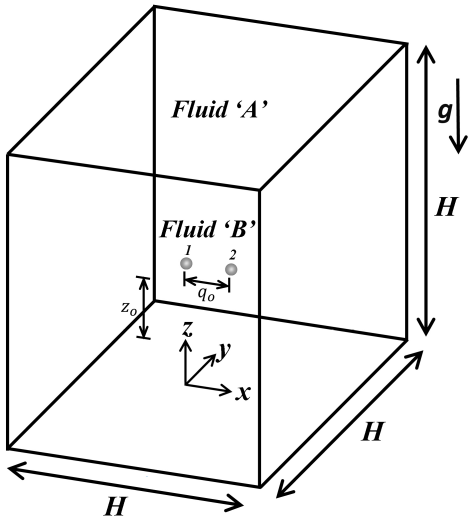

FIG. 2. Schematic diagram showing the initial configuration of two initially spherical drops (fluid 'B') rising in a surrounding medium (fluid 'A'). A cubic computational domain of size $H \times H \times H$ is used and the drops are placed at $(q_0/2, 0, z_0)$ and $(-q_0/2, 0, z_0)$. In the present study, $H = 120R$ and $z_0 = 7R$. The acceleration due to gravity (g) acts in the negative z direction.

The dynamics of the drops is governed is by the mass and momentum conservation, which are given by

$$\nabla \cdot \mathbf{u} = 0, \tag{1}$$

$$\rho \left[\frac{\partial \mathbf{u}}{\partial t} + \mathbf{u} \cdot \nabla \mathbf{u} \right] = -\nabla p + \nabla \cdot \left[\mu (\nabla \mathbf{u} + \nabla \mathbf{u}^T) \right] + \delta(\mathbf{x} - \mathbf{x}_\mathrm{f}) \sigma \kappa \mathbf{n} - \rho g \mathbf{j}, \tag{2}$$

where, $\mathbf{u} = (u, v, w)$ denotes the velocity field; u, v and w represent the velocity components in the x, y and z directions, respectively; p is the pressure field; t denotes time; $\mathbf{j}$ denotes the unit vector along the vertical direction; $\delta(\mathbf{x} - \mathbf{x}_\mathrm{f})$ is the delta distribution function (denoted by δ hereafter) whose value is zero everywhere except at the interface $\mathbf{x} = \mathbf{x}_\mathrm{f}$; $\kappa = \nabla \cdot \mathbf{n}$ is the interfacial curvature, wherein $\mathbf{n}$ is the unit normal pointing towards the surrounding medium at the interface.

In addition, the interface separating the drops and the surrounding medium is tracked by solving an advection equation for the volume fraction of the continuous phase, c. Thus, $c = 0$ and 1 for the drops (fluid 'B') and surrounding fluid (fluid 'A'), respectively:

$$\frac{\partial c}{\partial t} + \mathbf{u} \cdot \nabla c = 0. \tag{3}$$

The density, ρ, and the viscosity, μ, are assumed to depend on c as

$$\rho = (1 - c)\rho_B + c\rho_A, \tag{4}$$

$$\mu = (1 - c)\mu_B + c\mu_A. \tag{5}$$

The following scaling is used to non-dimensionalise Eqs. (1) - (5):

$$(x, y, z) = R\,(\widetilde{x}, \widetilde{y}, \widetilde{z})\,,\ t = \widetilde{t}\sqrt{R/g},\ \mathbf{u} = \tilde{\mathbf{u}}\sqrt{gR},\ p = \rho_A g R \widetilde{p},\ \mu = \mu_A \widetilde{\mu},\ \rho = \rho_A \widetilde{\rho},\ \delta = \widetilde{\delta}/R, \tag{6}$$

where the tildes designate dimensionless quantities, which are dropped hereafter and all the variables presented below are in dimensionless form. The governing dimensionless equations are given by

$$\nabla \cdot \mathbf{u} = 0, \tag{7}$$

$$\frac{\partial \mathbf{u}}{\partial t} + \mathbf{u} \cdot \nabla \mathbf{u} = -\nabla p + \frac{1}{Ga} \nabla \cdot \left[\mu (\nabla \mathbf{u} + \nabla \mathbf{u}^T) \right] + (1 - \rho_r) \delta \frac{\nabla \cdot \mathbf{n}}{Eo} \mathbf{n} - \rho \mathbf{j}, \tag{8}$$

where the dimensionless density and dynamic viscosity are given by

$$\rho = (1 - c)\rho_r + c, \tag{9}$$

$$\mu = (1 - c)\mu_r + c. \tag{10}$$

A volume-of-fluid (VoF) method based Navier-Stokes flow solver, Basilisk, [43, 44] that incorporates a height-function based balanced-force continuum-surface-force formulation is used. A dynamic adaptive grid refinement is incorporated, which provides a large number of grid points/cells on the vortical and interfacial regions. A grid convergence test is presented in Appendix for typical sets of parameters. To minimise the wall effect a sufficiently big computational domain is considered. The free-slip and no-penetration conditions are imposed on all the boundaries of the computational domain. The numerical scheme is second-order accurate in space and time. The present numerical method is similar to the one used by Tripathi *et al.* [20], which has been validated extensively in our previous studies [45–48]. The details of the numerical method have not been presented here in order to avoid the repetition. The results obtained from the present numerical simulations are presented next.

III. RESULTS AND DISCUSSION

The main objective of the present work is to investigate the effect of viscosity and density ratios on the dynamics of two drops rising side-by-side. We begin the presentation of our results by summarising the rising dynamics of two air bubbles in a liquid, at extremely small density and viscosity ratios, as considered by Tripathi *et al.* [11] in Figs. 3(a) and (b) for $Ga = 20$ and $Ga = 40$, respectively. The rest of the parameters are $Eo = 3.996$, $q_0 = 3$, $\rho_r = 10^{-3}$ and $\mu_r = 10^{-2}$. In Figs. 3(a) and (b), we present the temporal evolutions of the separation distance between the bubbles, $q \equiv ((x_{CG2} - x_{CG1})^2 + (y_{CG2} - y_{CG1})^2 + (z_{CG2} - z_{CG1})^2)^{1/2}$ (first row); the variations of the aspect ratio, A_r of bubble '1' and also that of a single bubble versus z, as well as the shapes of bubbles (x-z view) at different time instances and the corresponding z locations (second row); the top view of the trajectories of the two bubbles and the corresponding trajectory of the single bubble (third row); the contours of the z component of the vorticity ($\omega_z = \pm 0.02$) for the single and two bubbles cases at $t = 40$ (fourth row). Here, $(x_{CG1}, y_{CG1}, z_{CG1})$ and $(x_{CG2}, y_{CG2}, z_{CG2})$ are the positions of the centre of gravity of the bubbles at any time t. It can be seen that in this range of parameters, a single bubble initially flattens out as it rises, and shows path oscillations at a moderate Galilei number (see second and third rows). Shape oscillations are accompanied by path oscillations. Two bubbles rising side-by-side show the same behaviour, besides increasing their mutual separation as they rise (first row). It is to note that the two bubbles interact significantly with each other. This is seen by the fact that the vortex shedding is perfectly out-of-phase (fourth row in Fig. 3). In the third row of Fig. 3 (see the directions of arrows), it can also be observed that the paths of the left and right bubbles are symmetrical for $Ga = 20$, but they are asymmetrical for $Ga = 40$. Further investigation is required to understand this phenomenon.

We now ask what happens when we increase the density ratio significantly, namely the drops and surrounding liquid have densities of the same order of magnitude as each other. For this, the value of density ratio, ρ_r is varied from 0.05 to 0.95. We also increase the viscosity ratio, considering two cases (i) where the drop is ten times less viscous than the surrounding fluid ($\mu_r = 0.1$), (ii) where it is ten times more viscous than the surrounding fluid ($\mu_r = 10$). In Figs. 1(a) and (b), the viscosity and density ratios associated with the real fluid pairs are presented. For example, (μ_r, ρ_r) = (0.1,0.5), (0.1,0.95) and (10, 0.95) correspond to air-diethylether, diphenylether-isoeugenol and n-amylpthalate-diphenylether, respectively. The separation distance between the drops and shapes for different density ratios are shown in Figs. 4(a,c) and (b,d) for $\mu_r = 0.1$ and 10, respectively. The rest of the parameters are $Ga = 20$, $Eo = 3.996$ and $q_0 = 3$. As seen in the case of light bubbles (Fig. 3), drops with ρ_r varying from 0.05 to 0.95 too separate from each other increasingly as they rise. In other words, the horizontal forces are large enough to move heavy drops as well. Interestingly we see that the separation for the less viscous drops (Fig. 4a) varies non-monotonically with the density ratio. This can be explained by the interplay of horizontal forces and gravitational forces, by means of Fig. 5 below. Moreover the more viscous drops (Fig. 4b) seem to display greater horizontal motion if they are heavier (with increasing ρ_r). We shall return to this as well. The aspect ratio behaves along expected lines. If gravity were to be the primary driver of shape change, we would expect the shape to be more sensitive to the density ratio than to the viscosity ratio. We then expect a drop closer to the surrounding fluid in density to retain a more spherical shape than one which is significantly lighter. We see in Figs. 4 (c) and (d) that these expectations are borne out. Drops of density 0.95 times that of the surroundings remain practically spherical as they rise. For a hundred-fold change in viscosity, there is hardly any change in shape, as seen by comparing the density ratios 0.95 and 0.5 in Figs. 4(c) and (d). A non-monotonicity with density ratio is noticed at high drop viscosity (Fig. 4(d)) in the aspect ratio as well, which is discussed below. Though a drop's viscosity does not change its shape, the trajectories do differ. We thus conclude that the separation between the pair of drops is not driven by shape change, though it is modified by it.

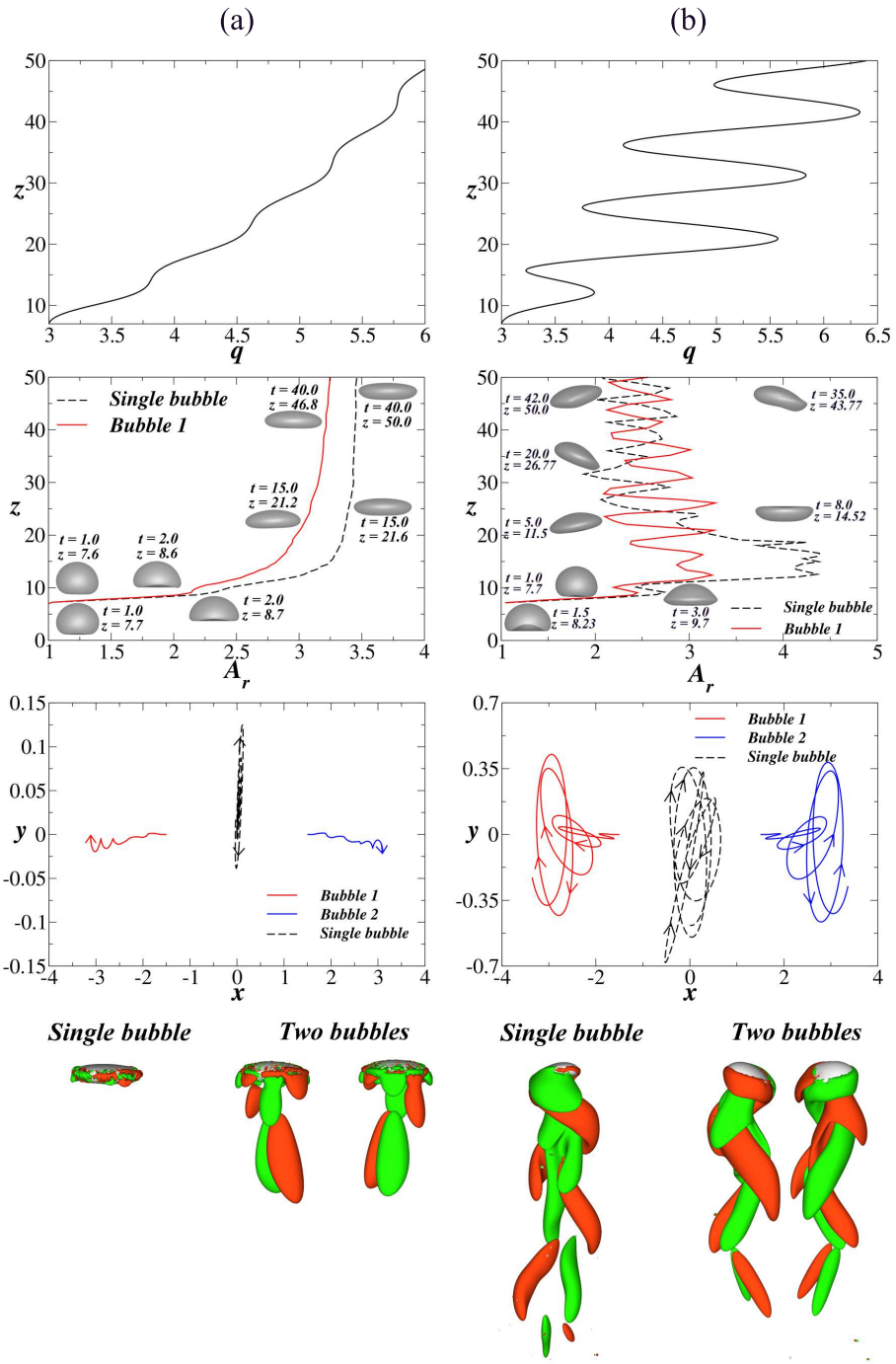

FIG. 3. This figure summarises earlier work [11], restricted to very light bubbles of very low viscosity. Evolution of the separation distance, q (first row). The aspect ratio, A_r of bubble '1' and also that of a single bubble versus z, as well as the shapes of bubble '1' (left side shapes) (x-z view) and the shapes of a single bubble (right side shapes) at different time instances and the corresponding z locations are shown (second row). The top view of the trajectories of the two bubbles and the corresponding trajectory of the single bubble (third row). Contours of the z component of the vorticity ($\omega_z = \pm 0.02$) for the single and two bubbles cases at $t = 40$ (fourth row). (a) $Ga = 20$ and (b) $Ga = 40$. The rest of the parameters are $Eo = 3.996$, $q_0 = 3$, $\rho_r = 10^{-3}$ and $\mu_r = 10^{-2}$.

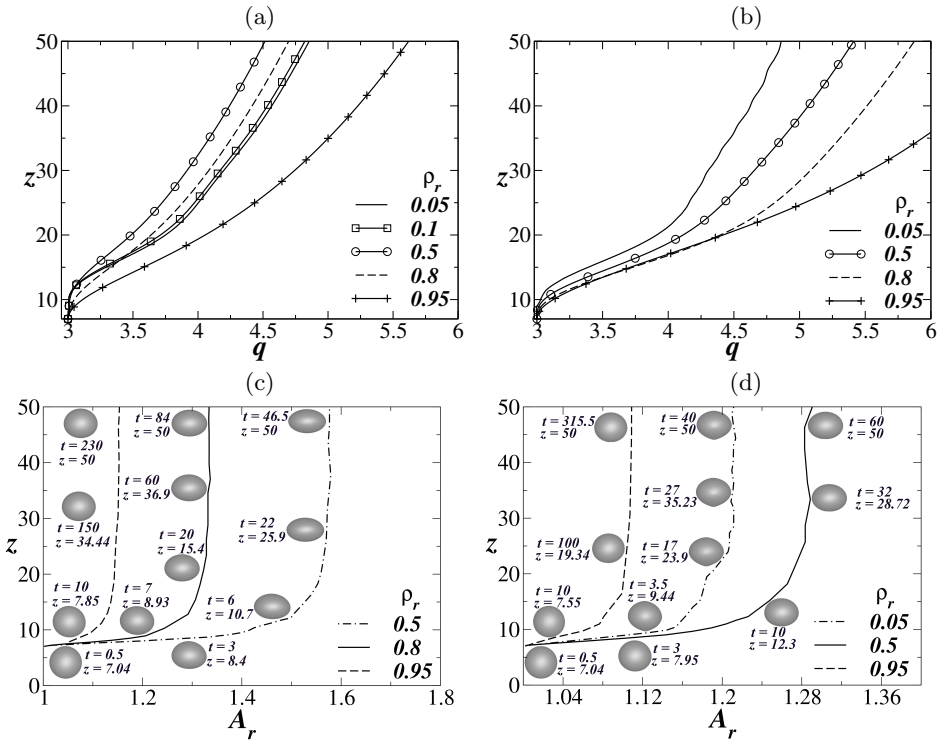

FIG. 4. Variations of (a,b) the separation distance between the drops, q and (c,d) the aspect ratio, A_r of drop '1' with z for different values of the density ratio, ρ_r. (a,c) $\mu_r = 0.1$ and (b,d) $\mu_r = 10$. The rest of the parameters are $Ga = 20$, $Eo = 3.996$ and $q_0 = 3$.

Figs. 5(a)-(f) are aimed at explaining the trends seen in Fig. 4. The velocity component of the centroid of drop '1' in the x direction (u_{CG}) is shown for the low ($\mu_r = 0.1$) and high viscosity ($\mu_r = 10$) drops, respectively in Figs. 5(a) and (b) for different density ratios. The rest of the parameters too are the same as those used to generate Fig. 4. For both the viscosity ratios considered, as the density of the drop becomes closer to that of the surrounding fluid, the separation rate decreases. The corresponding variations of the vertical velocity of the centroids (w_{CG}) of drop '1' with time are shown in Figs. 5(c) and (d). It can be seen that w_{CG} decreases monotonically with increasing drops density, until at the density ratio of 0.95 it is rather small. The important thing to notice is that there is no non-monotonicity in the velocity components as density is varied. The trend is as would be physically expected. First, the lighter drops have a higher horizontal velocity than the heavier drops. Also, with an increase in density, the buoyancy reduces and the vertical velocity decreases. Notice that the density difference in the case of $\rho_r = 0.95$ is a quarter of that for $\rho_r = 0.8$. This is reflected in the Reynolds number, which is proportional to w_{CG}. Due to various other intervening physics, the Reynolds numbers do not differ exactly by a factor of 4, but they are in a ratio close to this number. Thus, although all the drops in this figure have the same Galilei number, their inertia is actually very different. Since the velocity of the drop is proportional to the density difference between the two liquids, the inertia at $\rho_r = 0.95$ is far lower than that at $\rho_r = 0.8$. The viscosity of the drop again is seen to be of less consequence as compared to density, though one would expect that the drag on a higher viscosity drop would be higher because of higher internal shear and thus a more viscous drop should move up slower than a less viscous one. This effect is small but evident upon comparing w_{CG} in Figs. 5(c) and (d).

Now the separation between the drops at a given height (seen in Fig. 4) depends on the time taken to reach that height and the integral horizontal motion up to that time. Thus a heavier drop reaches a given height z at a much later time than a lighter drop, and the net horizontal separation distance between the drops is that attained over a much longer time, and so can be larger. As to the non-monotonicity, it happens as a consequence of the different rates at which u_{CG} and w_{CG} decrease with time as the density of the drops increases. This is made evident in Figs. 5(e) and (f), which show, respectively for low and high drop viscosity, the ratio u_{CG}/w_{CG}, which is an indication of the angle of separation of the drops. Clearly at $\rho_r = 0.95$, there is a crossover. It is to be noted that the buoyancy at $\rho_r = 0.95$ is only a fourth of that at $\rho_r = 0.8$, resulting in a drastic reduction in the vertical velocity. The horizontal velocity too is reduced but the ratio of the two is dramatically changed. Note that the horizontal velocities are much lower than the vertical. The out-of-plane velocity (not shown) is negligible in these cases, so the motion is two-dimensional. Also close inspection of Figs. 5(a-b) and (e-f) reveals that as the separation distance between the drops becomes large at

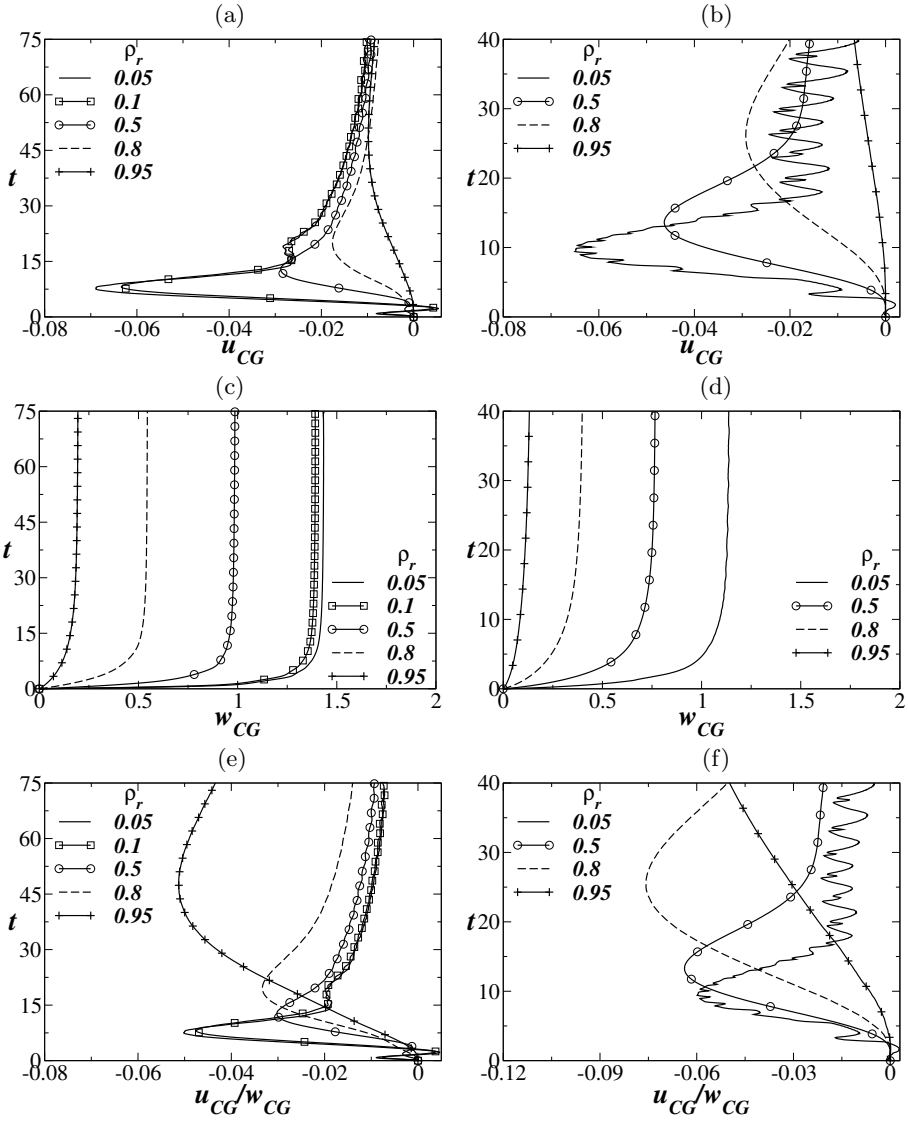

FIG. 5. Variations of velocity of the centroid of drop '1' in (a,b) the x direction (u_{CG}), (c,d) the z direction (w_{CG}) and (e.f) u_{CG}/w_{CG} of drop '1' with time for different values of the density ratio, ρ_r. (a,c,e) $\mu_r = 0.1$ and (b,d,f) $\mu_r = 10$. The rest of the parameters are $Ga = 20$, $Eo = 3.996$ and $q_0 = 3$.

later times they stop influencing each other and behave like single drops. It can be seen that at late times, u_{CG} and u_{CG}/w_{CG} approach towards zero, indicating that the lateral migration of the drops has been reduced.

The next question which arises is whether the findings above are universal for any Galilei number. The variations of the separation distance between the drops, q with z for different values of the density ratio, ρ_r for a higher Galilei number ($Ga = 40$) are shown in Figs. 6(a) and (b) for $\mu_r = 0.1$ and $\mu_r = 10$, respectively. The rest of the parameters remain the same as in Fig. 4. For $Ga = 40$, a pair of much lighter and less viscous drops ($\rho_r = 0.05$ and $\mu_r = 0.1$), undergo significantly large path oscillations. In fact, the dynamics of the drops is three-dimensional in this case (Fig. 6(a)). These oscillations are suppressed with an increase in the density ratio. At $\rho_r = 0.95$, a pair of less viscous drops move away from each other smoothly as they rise. The amplitude of oscillations observed at low density ratios is smaller for high viscous drops (Fig. 6(b)). Thus very light drops behave in a manner similar to bubbles. Close inspection also reveals that the wavelength of these oscillations increases with the increase in the viscosity ratio. A non-monotonic trend in the variation of the separation distance can be seen in Fig. 6(b) on either side of $\rho_r = 0.8$. This can be explained by the arguments offered above in our discussion of fig. 5.

Figs. 7(a)-(c) are for very light drops ($\rho_r = 10^{-3}$) of viscosity less than that of the surrounding fluid, to study the effect of changing the viscosity over four orders of magnitude. For $\mu_r < 1$, Fig. 7 (a) shows that as the drops' viscosity increases, their tendency to wobble increases as well. The trajectories of the two drops rising side-by-side, along with

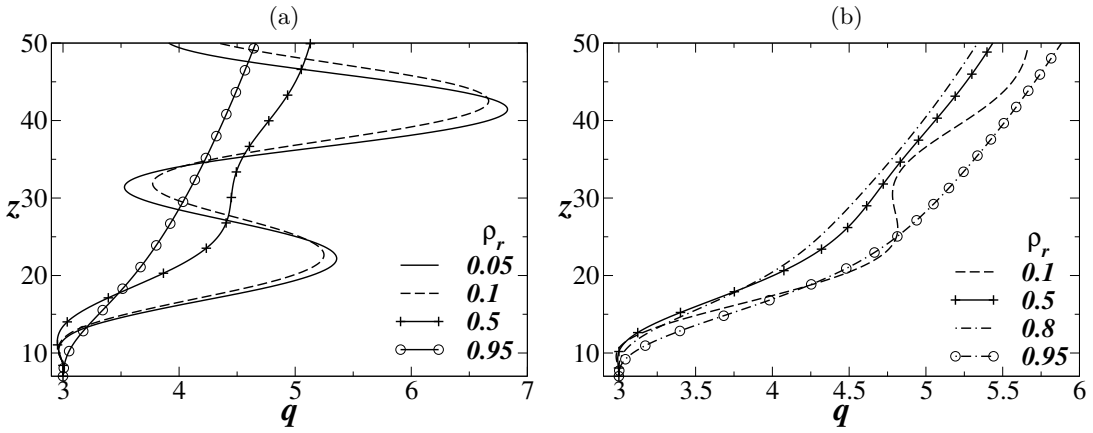

FIG. 6. Variations of the separation distance, q with z for different values of the density ratio, ρ_r. (a,) $\mu_r = 0.1$ and (b) $\mu_r = 10$. The rest of the parameters are $Ga = 40$, $Eo = 3.996$ and $q_0 = 3$.

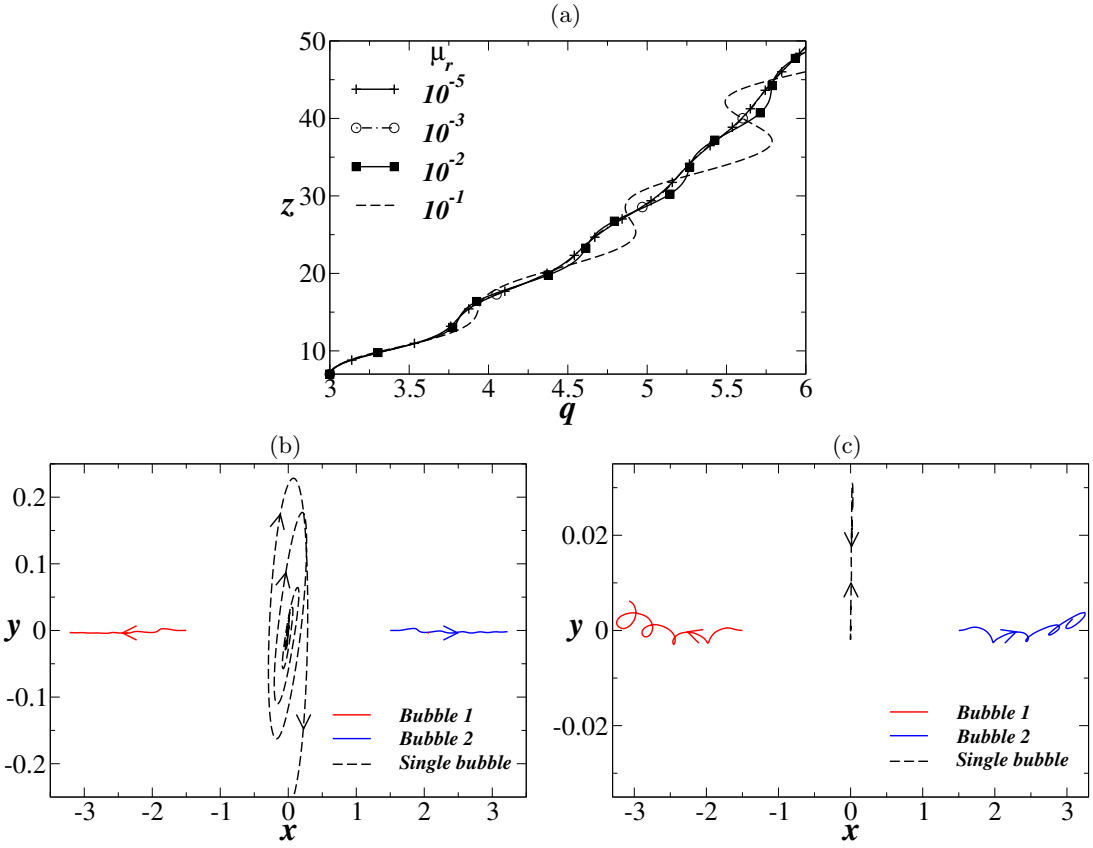

FIG. 7. (a) Variations of the separation distance, q versus z for different values of μ_r, the top view of the trajectories of the two drops and the corresponding trajectory of the single drop for (b) $\mu_r = 10^{-5}$ and (c) $\mu_r = 10^{-1}$. The rest of the parameters are $Ga = 20$, $Eo = 3.996$, $q_0 = 3$ and $\rho_r = 10^{-3}$.

the trajectories of the single drop in the x-y plane (top view) for $\mu_r = 10^{-5}$ and $\mu_r = 10^{-1}$ are shown in Figs. 7 (b) and (c), respectively. The gentle wobble in the x-z plane for the drops of relatively higher viscosity is seen in Fig. 7 (c) to correspond to a small-amplitude spiral in the x-y plane. However, for the entire range of viscosity ratios, it is seen that y remains small, so the dynamics of the drop is restricted to two dimensions. This is seen to be totally unlike the dynamics of a single drop, which is highly three-dimensional, in fact spiralling at very low drop viscosity ($\mu_r = 10^{-5}$). At higher drop viscosity ($\mu_r = 10^{-1}$), a single drop is restricted to two dimensions, but instead in the y-z plane, oscillating back and forth in y as it rises in z. Thus, while the single drop dynamics is very sensitive to

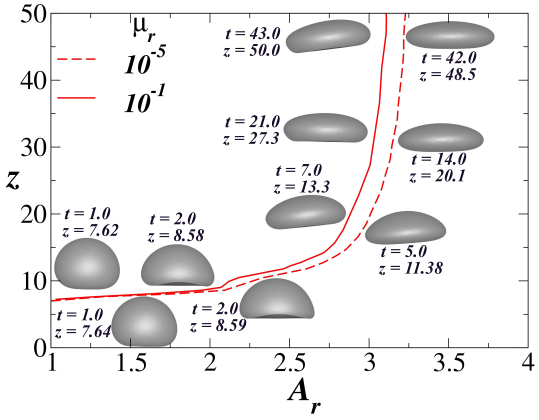

FIG. 8. Variations of the aspect ratio, A_r of drop '1' versus z for different values of μ_r. The rest of the parameters are the same as Fig. 7.

drop viscosity in this range of parameters, two drops dynamics is not. Fig. 8 shows the variation of the aspect ratio of drop '1' with height in this viscosity ratio range, and it is seen that the aspect ratio too is not sensitive to viscosity ratio.

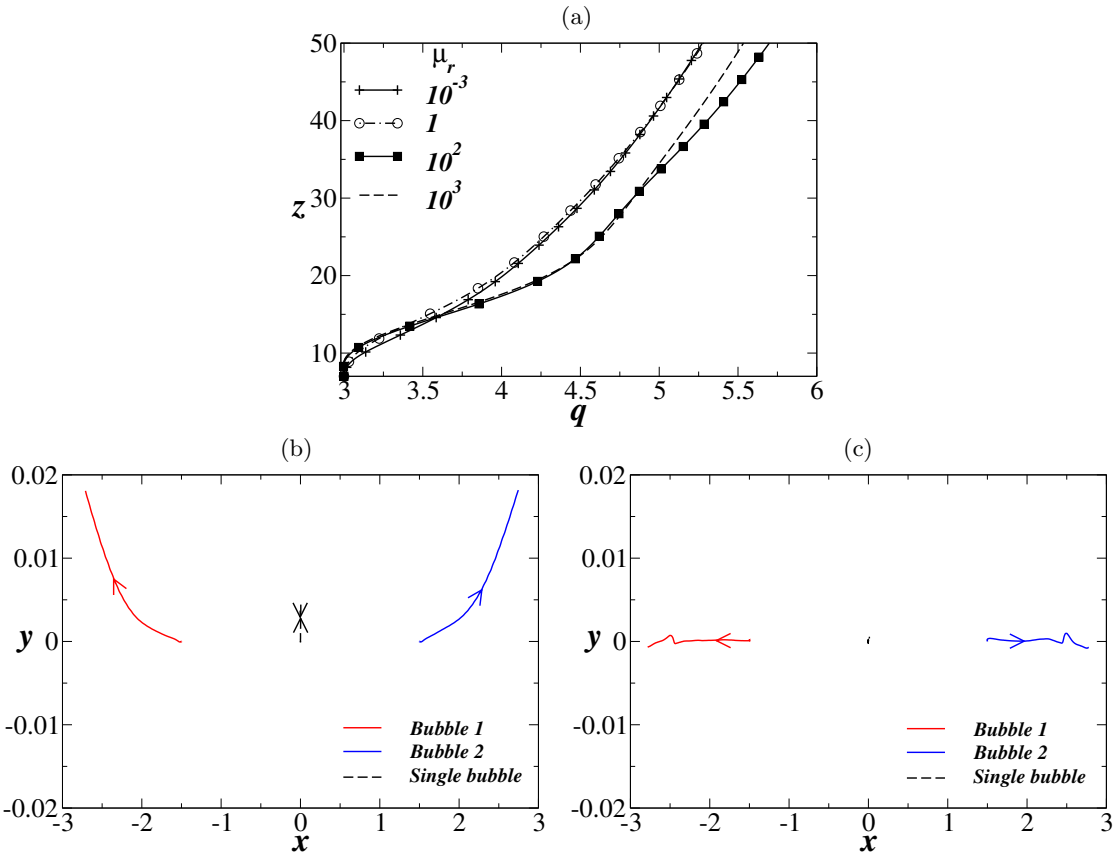

FIG. 9. (a) Variations of the separation distance, q versus z for different values of μ_r, the top view of the trajectories of the two drops and the corresponding trajectory of the single drop for (b) $\mu_r = 10^{-3}$ and (c) $\mu_r = 10^3$. The rest of the parameters are $Ga = 20$, $Eo = 3.996$, $q_0 = 3$ and $\rho_r = 0.5$.

Figs. 9 and 10 are the counterparts of Figs. 7 and 8 but for a heavier drop than before ($\rho_r = 0.5$). A big range of viscosity ratios is considered. Now the single drop dynamics is much simpler than before. On the other hand, a heavier pair of drops displays three-dimensional behaviour at low viscosity ($\mu_r = 10^{-3}$) and two dimensional behaviour at

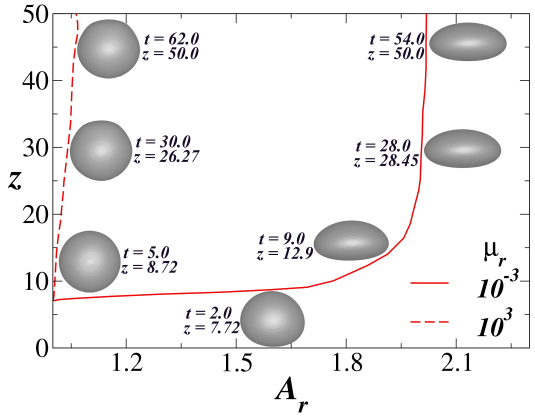

FIG. 10. Variations of the aspect ratio, A_r of drop '1' versus z for different values of μ_r. The rest of the parameters are the same as Fig. 9.

high viscosity ($\mu_r = 10^3$), where the separation distance between the drops increases as they rise, just as for a pair of solids [41, 42]. As seen before, the high viscosity drop is practically spherical (see Fig. 10). Since the shape is nearly spherical, the mechanism described by Legendre *et al.* [7] for the viscous case, as summarised in the introduction section above, is applicable here as well. Thus, the drops move away from each other as time progresses. Thus one expects vortical effects to be strong within the drop for $\mu_r \ll 1$ and around the drop for $\mu_r \gg 1$. The interaction of vorticity for $\mu_r \gg 1$ drives the drops away from each other, while for $\mu_r \ll 1$, they remain closer to each other. Decreasing the viscosity ratio also increases the ability of the drop to deform for a fixed set of other parameters, which can be seen in Fig. 10. In other words, a more viscous drop requires more time to deform as compared to a less viscous drop. We notice however that the effect of changing viscosity by many orders of magnitude is surprisingly small.

These findings show that knowing the manner in which single-drop dynamics differs from that of a pair of drops in one parameter range tells us nothing about what happens in another range. Each parameter changes the dynamics in ways that at this point only the simulations tell us. We cannot easily make apriori predictions from physical considerations. A lot needs to be understood and explained, as well as checked experimentally.

IV. CONCLUDING REMARKS

The rise dynamics of a side-by-side pair of drops is investigated via three-dimensional numerical simulations, using a volume-of-fluid method based Navier-Stokes flow solver with dynamic adaptive grid refinement feature for the vortical and interfacial regions [43, 44]. A big computational domain is considered such that boundary effects are negligible. Although the dynamics of gas bubbles rising in liquids and the behaviour of a single drop in systems with high and low density contrasts have been investigated extensively, two liquid drops rising in a surrounding liquid, with the same order of magnitude of density, has not been investigated yet in spite of the fact that one can encounter liquid-liquid systems in many industrial applications. This, therefore, dictates the choice of the wide range of density and viscosity ratios we study.

It is known that two air bubbles rising side-by-side in a liquid at low Ga tend to separate as they rise, due to interactions between the two boundary layers. The present study reports interesting dynamics, opposite to that of a single air bubble, that occurs when we increase the density of the bubble even in the case of low inertia. For $Ga = 20$, while a single air bubble rises in a straight path, a pair of air bubbles displays three-dimensional motion and the separation between the bubbles increases. Even when we increase the density of the drop (in liquid-liquid systems), the horizontal forces are still large enough to move apart the heavy drops. When the viscosity of the drops is less than that of the surrounding fluid, the separation distance between the drops exhibits a non-monotonic trend with the increase in the density ratio. This is a consequence of the different rates at which x and z velocity components of the drops decrease with time as the density of the drops increases.

Increasing inertia (Ga) increases path oscillations significantly; these oscillations decrease as the drop density approaches that of the surrounding fluid. It is also observed that the wavelength of these oscillations increases with an increase in the viscosity ratio. The non-monotonic trend in the variation of the separation distance is also evident at high Ga, but at a higher density ratio.

In the case of light drops, the pair lives in two dimensions, and increasing drop viscosity decreases their tendency to

wobble while the trajectories are still planar. This is in contrast with the dynamics of a single drop, whose trajectory is highly three-dimensional at low drop viscosity, but restricted to two dimensional motion at higher drop viscosity. This result reveals that while single drop dynamics is very sensitive to drop viscosity, two drop dynamics is not, at least for the range of parameters considered in the present study. In contrast, a heavier pair of drops displays three-dimensional behaviour at low viscosity and two-dimensional behaviour at high viscosity of the drops. These drops also move apart. The separation behaviour for high drop viscosity is similar to that of a pair of solids, as described above. Increasing viscosity of the drops makes them more spherical. The observation that drops of the same shape can differ in their trajectories reveals that the separation between a pair of drops is not driven by shape change, though it is modified by it. This is in contrast to gas-liquid systems, where the nonlinear dynamics of bubbles trajectory is tied to their deformation.

By varying the viscosity ratio by many orders of magnitude we have learned that changes in the dynamics of a pair of drops are far more sensitive to changes in the density ratio between the drops and their surroundings than to viscosity ratio. We have also seen that the tendency for two drops at low inertia to drift apart is universal across density and viscosity ratios and at different levels of inertia.

APPENDIX

We have conducted grid convergence test for two extreme viscosity ratios. In Figs. 11(a) and (b), the shapes of two air bubbles at $t = 9$ rising in a liquid with $\mu_r = 10^{-5}$ obtained using the smallest grid size, $\Delta = 0.058$ and $\Delta = 0.029$ are presented, respectively. The rest of the parameters are the same as those of Fig. 7. The separation distance between the bubbles (q) and the aspect ratios of bubble '1' (A_{r1}) and bubble '2' (A_{r2}) at this time are also shown in each panel. Similarly, the shapes, their separation distance, q and the aspect ratios of two liquid drops rising in another liquid with $\mu_r = 10^3$ are presented in Fig. 12. The rest of the parameters are the same as those of Fig. 9. It can be seen that even for these extreme viscosity ratios halving the smallest grid size gives a difference only in the second decimal place. Thus $\Delta = 0.058$ is used to generate the results presented in this study.

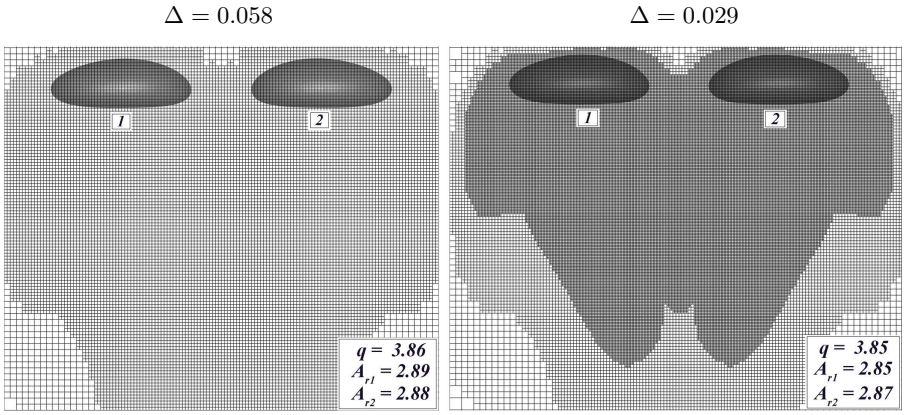

FIG. 11. The grid convergence test showing the bubble shapes at $t = 9$ for $\mu_r = 10^{-5}$ with the rest of the parameters the same as those used to generate Fig. 7(b). The values of the separation distance, q, the aspect ratios of drops '1' and '2' (designated below the bubbles) obtained for $\Delta = 0.058$ and $\Delta = 0.029$ are given in each panel.

ACKNOWLEDGEMENTS

KS thanks Department of Science & Technology, India for providing financial support through the grant number, MTR/2017/000029. We also thank the anonymous referees for comments that were most helpful in improving this paper.

[1] W. D. Deckwer, *Bubble Column Reactors* (Wiley, New York, 1992).

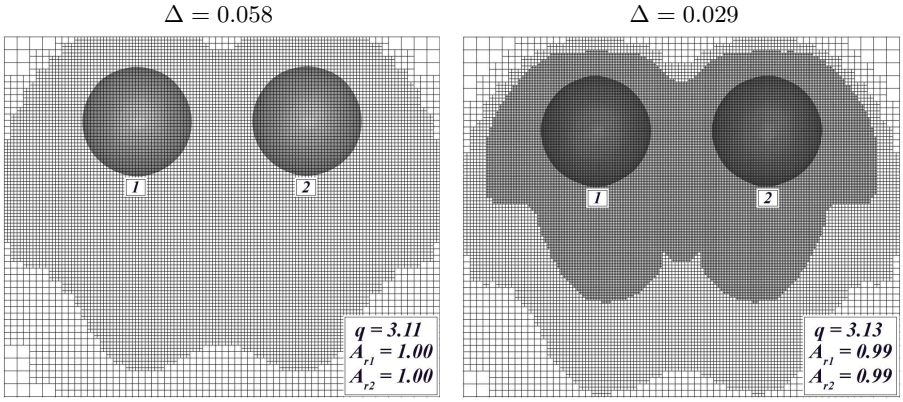

FIG. 12. The grid convergence test showing the drop shapes at $t = 9$ for $\mu_r = 10^3$ with the rest of the parameters the same as those used to generate Fig. 9(a). The values of the separation distance, q, the aspect ratios of drops '1' and '2' (designated below the drops) obtained for $\Delta = 0.058$ and $\Delta = 0.029$ are given in each panel.

[2] B. Aboulhasanzadeh and G. Tryggvason, "Effect of bubble interactions on mass transfer in bubbly flow," Int. J. Heat Mass Transfer **79**, 390–396 (2014).

[3] K. Hiroaki and S. Toshiyuki, "Influence of surfactants on the motion of a pair of bubbles in quiescent liquids," Japanese Journal of Multiphase Flow **29**, 515–522 (2016).

[4] B. Bunner and G. Tryggvason, "Direct numerical simulations of three-dimensional bubbly flows," Phys. Fluids **11**, 1967–1969 (1999).

[5] T. Bonometti, J. Magnaudet, and P. Gardin, "On the dispersion of solid particles in a liquid agitated by a bubble swarm," Metall. Mater. Trans. B **38**, 739–750 (2007).

[6] JC Cano-Lozano, P Bohorquez, and C Mart´inez-Bazán, "Wake instability of a fixed axisymmetric bubble of realistic shape," Int. J. Multiphase Flow **51**, 11–21 (2013).

[7] D. Legendre, J. Magnaudet, and G. Mougin, "Hydrodynamic interactions between two spherical bubbles rising side by side in a viscous liquid," J. Fluid Mech. **497**, 133–166 (2003).

[8] T. Sanada, A. Sato, M. Shirota, and M. Watanable, "Motion and coalescence of a pair of bubbles rising side by side," Chem. Eng. Sci. **64**, 2659–2671 (2009).

[9] Y. Hallez and D. Legendre, "Interaction between two spherical bubbles rising in a viscous liquid," J. Fluid Mech. **673**, 406–431 (2011).

[10] I. Chakraborty, G. Biswas, and P. S. Ghoshdastidar, "A coupled level-set and volume-of-fluid method for the buoyant rise of gas bubbles in liquids," Int. J. Heat Mass Transfer **58**, 240–259 (2013).

[11] M. K. Tripathi, A. R. Premlata, K. C. Sahu, and R. Govindarajan, "Two initially spherical bubbles rising in quiescent liquid," Phys. Rev. Fluids **2**, 073601 (2017).

[12] M. Manga and H. A. Stone, "Buoyancy-driven interactions between two deformable viscous drops," J. Fluid Mech. **256**, 647–683 (1993).

[13] H. Yuan and A. Prosperetti, "On the in-line motion of two spherical bubbles in a viscous fluid," J. Fluid Mech. **278**, 325–349 (1994).

[14] J. M. Boulton-Stone, P. B. Robinson, and J. R. Blake, "A note on the axisymmetric interaction of pairs of rising, deforming gas bubbles," Int. J. Multiphase Flow **22**, 122–123 (1996).

[15] A. Gupta and R. Kumar, "Lattice boltzmann simulation to study multiple bubble dynamics," Int. J. Heat Mass Transf. **51**, 5192–5203 (2008).

[16] R. H. Chen, W. X. Tian, G. H. Su, S. Z. Qiu, Y. Ishiwatari, and Y. Oka, "Numerical investigation on coalescence of bubble pairs rising in a stagnant liquid," Chem. Eng. Sci. **66**, 5055–5063 (2011).

[17] H. Kusuno, H. Yamamoto, and T. Sanada, "Lift force acting on a pair of clean bubbles rising in-line," Phys. Fluids **31**, 072105 (2019).

[18] D. Bhaga and M. E. Weber, "Bubbles in viscous liquids: shapes, wakes and velocities," J. Fluid Mech. **105**, 61–85 (1981).

[19] W. L. Haberman and R. K. Morton, *An experimental investigation of the drag and shape of air bubbles rising in various liquids*, Tech. Rep. (DTIC Document, 1953).

[20] M. K. Tripathi, K. C. Sahu, and R. Govindarajan, "Dynamics of an initially spherical bubble rising in quiescent liquid," Nat. Commun. **6**, 6268 (2015).

[21] D. M. Sharaf, A. R. Premlata, M. K. Tripathi, B. Karri, and K. C. Sahu, "Shapes and paths of an air bubble rising in quiescent liquids," Phys. Fluids **29**, 122104 (2017).

[22] M. Sussman and E. G. Puckett, "A coupled level set and volume-of-fluid method for computing 3D and axisymmetric incompressible two-phase flows," J. Comput. Phys **162**, 301–337 (2000).

[23] W. Dijkhuizen, M. van Sint Annaland, and J. A. M. Kuipers, "Numerical and experimental investigation of the lift force on single bubbles," Chem. Eng. Sci. **65**, 1274–1287 (2010).

[24] M. W. Baltussen, J. A. M. Kuipers, and N. G. Deen, "A critical comparison of surface tension models for the volume of fluid method," Chem. Eng. Sci. **109**, 65–74 (2014).

[25] G. Mougin and J. Magnaudet, "Path instability of a rising bubble," Phys. Rev. Lett. **88**, 014502 (2002).

[26] A. Tomiyama, G. P. Celata, S. Hosokawa, and S. Yoshida, "Terminal velocity of single bubbles in surface tension force dominant regime," Int. J. Multiphase Flow **28**, 1497–1519 (2002).

[27] C. Veldhuis, Biesheuvel A., and L. van Wijngaarden, "Shape oscillations on bubbles rising in clean and in tap water," Phys. Fluids **20**, 040705 (2008).

[28] L. G. Leal, *Laminar Flow and Convective Transport Processes* (Butterworth and Heinemann, Stoneham, MA, 1992).

[29] J. B. W. Kok, "Dynamics of a pair of gas bubbles moving through liquid. part I. Theory." Eur. J. Mech. B/Fluids **12**, 515–540 (1993).

[30] J. Zhang, L. Chen, and M.-J. Ni, "Vortex interactions between a pair of bubbles rising side by side in ordinary viscous liquids," Phys. Rev. Fluids **4**, 043604 (2019).

[31] P. C. Duineveld, "Bouncing and coalescence of bubble pair rising at high Reynolds number in pure water or aqueous surfactant solutions," Appl. Sci. Res. **58**, 409–439 (1998).

[32] J. R. Velez-Cordero, P. Diego, S. amd Yue, J. J. Feng, and R. Zenit, "Hydrodynamic interaction between a pair of bubbles ascending in shear-thinning inelastic fluids," J. Non Newt. Fluid Mech. **166**, 118–132 (2011).

[33] Md. T. Islam, P. Ganesan, and J. Cheng, "A pair of bubbles rising dynamics in a xanthan gum solution: a CFD study," RSC Adv. **5**, 7819–7831 (2015).

[34] R. Zenit and J. J. Feng, "Hydrodynamic interactions among bubbles, drops, and particles in non-Newtonian liquids," Ann. Rev. Fluid Mech. **50** (2018).

[35] J. B. W. Kok, "Dynamics of a pair of gas bubbles moving through liquid. part II. Experiment." Eur. J. Mech. B/Fluids **12**, 541–560 (1993).

[36] D. D. Joseph, Y. J. Liu, M. Poletto, and J. Feng, "Aggregation and dispersion of spheres falling in viscoelastic liquids," J. Non Newt. Fluid Mech. **54**, 45–86 (1994).

[37] M. Ohta, S. Yamaguchi, Y. Yoshida, and M. Sussman, "The sensitivity of drop motion due to the density and viscosity ratio," Phys. Fluids **22**, 072102 (2010).

[38] M. Ohta, Y. Akama, Y. Yoshida, and M. Sussman, "Influence of the viscosity ratio on drop dynamics and breakup for a drop rising in an immiscible low-viscosity liquid," J. Fluid Mech. **752**, 383–409 (2014).

[39] L. Liu, H. Tang, and S. Quan, "Shapes and terminal velocities of a drop rising in stagnant liquids," Computers & Fluids **81**, 17–25 (2013).

[40] A. R. Premlata, M. K. Tripathi, and K. C. Sahu, "Dynamics of rising bubble inside a viscosity-stratified medium," Phys. Fluids **27**, 072105 (2015).

[41] R. Folkersma, H. N. Stein, and F. N. Van de Vosse, "Hydrodynamic interactions between two identical spheres held fixed side by side against a uniform stream directed perpendicular to the line connecting the spheres centres," Int. J. Multiphase Flow **26**, 877–887 (2000).

[42] I. Kim, S. Elghobashi, and W. A. Sirignano, "Three-dimensional flow over two spheres placed side by side," J. Fluid Mech. **246**, 465–488 (1993).

[43] S. Popinet, "Gerris: a tree-based adaptive solver for the incompressible euler equations in complex geometries," J. Comput. Phys **190**, 572–600 (2003).

[44] S. Popinet, "An accurate adaptive solver for surface-tension-driven interfacial flows," J. Comput. Phys **228**, 5838–5866 (2009).

[45] A. R. Premlata, M. K. Tripathi, B. Karri, and K. C. Sahu, "Dynamics of an air bubble rising in a non-Newtonian liquid in the axisymmetric regime," J. Non Newt. Fluid Mech. **239**, 53–61 (2017).

[46] M. K. Tripathi, K. C. Sahu, G. Karapetsas, and O. K. Matar, "Bubble rise dynamics in a viscoplastic material," J. Non Newt. Fluid Mech. **222**, 217–226 (2015).

[47] M. K. Tripathi, K. C. Sahu, G. Karapetsas, K. Sefiane, and O. K. Matar, "Non-isothermal bubble rise: non-monotonic dependence of surface tension on temperature," J. Fluid Mech. **763**, 82–108 (2015).

[48] M. K. Tripathi, K. C. Sahu, and R. Govindarajan, "Why a falling drop does not in general behave like a rising bubble," Sci. Rep. **4**, 4771 (2014).